# SGN-LIV1A: A Novel Antibody-Drug Conjugate Targeting LIV-1 for the Treatment of Metastatic Breast Cancer

Django Sussman*, Leia M. Smith, Martha E. Anderson, Steve Duniho, Joshua H. Hunter, Heather Kostner, Jamie B. Miyamoto, Albina Nesterova, Lori Westendorf, Heather A. Van Epps, Nancy Whiting, Dennis R. Benjamin

Seattle Genetics, Inc. Bothell, WA, USA

* Corresponding author
Django Sussman, Ph.D.
Seattle Genetics, Inc.
21823 30th Drive SE, Bothell, USA
Phone: +1-425-527-4630
Email: dsussman@seagen.com

**Running Title:** Antibody-Drug Conjugate Targeting LIV-1 for Breast Cancer

**Key words:** Antibody-Drug conjugate, Breast Cancer, Targeted therapy, LIV-1

**Abreviations:** ADC, anti-body drug conjugate; CDR, complementarity-determining Region; EMT, epidermal-to-mesenchymal transition; ER, estrogen receptor; MMAE, monomethylauristatin E; PgR, progesterone receptor

**Conflict of interest statement:** The authors were Seattle Genetics employees with ownership interests in this company at the time that this work was undertaken.

**There was no grant support for the work described in this manuscript**

**Other notes:**
Word count of manuscript: ~4,400
4 figures
3 tables

**ABSTRACT**

In this manuscript we describe a novel antibody-drug conjugate (SGN-LIV1A), targeting the zinc transporter LIV-1 (SLC39A6) for the treatment of metastatic breast cancer. LIV-1 was previously known to be expressed by estrogen receptor-positive breast cancers. In this study, we show that LIV-1 expression is maintained after hormonal therapy in primary and metastatic sites and is also up regulated in triple-negative breast cancers. In addition to breast cancer, other indications showing LIV-1 expression include melanoma, prostate, ovarian and uterine cancer. SGN-LIV1A consists of a humanized antibody conjugated through a proteolytically cleavable linker to monomethylauristatin E, a potent microtubule-disrupting agent. When bound to surface-expressed LIV-1 on immortalized cell lines, this ADC is internalized and traffics to the lysozome. SGN-LIV1A displays specific *in vitro* cytotoxic activity against LIV-1 expressing cancer cells. *In vitro* results are recapitulated *in vivo* where antitumor activity is demonstrated in tumor models of breast and cervical cancer lineages. These results support the clinical evaluation of SGN-LIV1A as a novel therapeutic agent for patients with LIV-1 expressing cancer.

## INTRODUCTION:

In the United States, nearly 300,000 women are diagnosed with breast cancer each year and it is the second leading cause of cancer related mortality in women. Surgery, radiation, hormone therapy and chemotherapy are effective treatments for many, but over 40,000 patients succumb to the disease annually. Breast cancers are classified on the basis of three protein expression markers: estrogen receptor (ER), progesterone receptor (PgR), and the over-expression of the growth factor receptor HER2/neu. Hormonal therapies, including tamoxifen and aromatase inhibitors, can be effective in treating tumors that express the hormone receptors ER and PgR. HER2-directed therapies are useful for tumors that express HER2/neu; these tumors are the only class of breast cancer that is currently eligible for immunotherapy. For these patients, unconjugated antibodies (Herceptin®, Perjeta®) are generally used in combination with chemotherapy. The treatment options for triple-negative breast tumors, those that do not express ER, PgR or HER2/neu, are restricted to chemotherapy, radiation and surgery. Additionally, there are limited effective treatment options available to patients with advanced stage disease with relatively poor survival rates of stage III patients (52%) and significantly worse for stage IV patients (15%). There is clearly a significant need for effective treatments for late stage breast cancer.

Antibody Drug Conjugates (ADCs) are a relatively new treatment modality that takes advantage of the exquisite specificity of monoclonal antibodies by using them to deliver a highly potent cytotoxic agent. The ADC described here is an anti-LIV-1 antibody linked via a cleavable dipeptide linker to monomethylauristatin E (MMAE), the cytotoxic agent. While there are at least twenty-one ADCs in clinical development (nine auristatin

based)(1), only one is approved for use in breast cancer (Kadcyla for HER2+ patient populations).

LIV-1 is a member of the solute carrier family 39; a multi-span transmembrane protein with putative zinc transporter and metalloproteinase activity (2, 3). It was first identified as an estrogen-induced gene in the breast cancer cell line ZR-75-1 (4). LIV-1 expression has been linked to epidermal-to-mesenchymal transition (EMT) in both normal vertebrate embryo development (5) and preclinical models (6-8) leading to malignant progression and metastasis. There is evidence of LIV-1 interacting with the transcription factors STAT3 and Snail to down-regulate expression of E-cadherin to promote EMT (9, 10). Expression is also associated with lymph node involvement in breast cancer (11). In addition to breast cancer, it has been detected in other neoplastic tissue types including pancreatic, prostate, breast, melanoma, cervical, and uterine (8, 12, 13). We evaluated LIV-1 expression in a number of indications using immunohistochemical analysis on tissue biopsies. In addition, we performed quantitative flow cytometry to determine expression of LIV-1 on a panel of cell lines derived from various cancer types. Using a humanized antibody specific for LIV-1 (hLIV22) conjugated to monomethyl auristatin E (14), we demonstrated ADC internalization, *in vitro* cytotoxicity and anti-tumor activity in *in vivo* breast and cervical cancer models.

## Materials and Methods

**Cell lines and culture. MCF-7 cells were obtained from 3 different sources: MCF-7 (ATCC® HTB-22™)** from the American Type Culture Collection (ATCC, Manassas, VA); MCF-7 DSMZ from Deutsche Sammlung von Mikroorganismen und Zellkulturen (DSMZ, Braunschweig, Germany) and MCF-7 NCI from NCI-Frederick Cancer Cell Line Repository (NCI-Frederick, MD). Other cell lines were from the American Type Culture Collection (ATCC, Manassas, VA) with the exception of PC-3 and HupT3 cells which were obtained from Deutsche Sammlung von Mikroorganismen und Zellkulturen (DSMZ, Braunschweig, Germany). All cell lines were received prior to 2010 and cultured according to supplier recommendations; cell lines used for *in vitro* cytotoxicity ((MCF-7 ATCC) and *in vivo* efficacy studies (MCF-7 NCI and HELA) were authenticated using the Cell Check service provided by IDEXX Bioresearch (identity confirmation by STR-based DNA profiling and multiplex PCR). A Chinese Hamster Ovary (CHO) cell line expressing human LIV-1 was generated by transfecting a CHO DG44 cell line with a plasmid coding for the intact LIV-1 gene. DHFR selection was used to identify positive clones.

**Antibody humanization.** The murine antibody mLIV22 specifically binds an epitope in the extracellular N-terminus (residues 1-329) of LIV-1. Complementarity-determining region (CDR) grafting was used to generate the humanized anti-LIV-1 antibody hLIV22. First, the mLIV22 VL CDRs (as defined by Kabat et al. (15)) were grafted on to the framework regions of human germline exons IGKV2-30 and JK4 obtained from NCBI and fused to human kappa constant domain. Likewise, the complementarity-determining

regions of mLIV22 VH were grafted onto the framework regions of human germline exons VH1-2 and JH5 fused to the human IgG1 constant domains. In addition, framework mutations, F36Y and R46P in the light chain and Y27L, F29I, T30E, S76N and R94V of the heavy chain (numbering scheme of Kabat et al.), were introduced into the humanized variable domains to enhance antigen-binding activity. The resultant humanized anti-LIV-1 antibody, hLIV22, showed comparable antigen-binding activity to mLIV22 in competition-binding assays using CHO cells transfected with LIV-1.

**Immunohistochemistry**

Formalin-fixed paraffin-embedded tumor samples were obtained from several sources: the Cooperative Human Tissue Network, (Rockville, MD, USA); Tissue Solutions (Glasgow, Scotland); NDRI (Philadelphia, PA, USA). Slides were deparaffinized and antigen retrieval was performed using EDTA based buffer. Samples were pre-blocked with non-serum protein block (Dako A/S, Glostrup, Denmark) and primary antibodies, used separately, were incubated for 45 minutes at room temperature. Anti-LIV-1 mAb and isotype control IgG were used at 1 μg/ml. Bond Polymer Refine Detection ( Leica Microsystems, Germany) was used for detection with 3,3′-diaminobenzidine as the substrate for horseradish peroxidase and Bond Polymer Refine Red Detection (Leica Microsystems, Germany) was used for detection with Fast Red as substrate for alkaline phosphatase. Slides were then scored using a qualitative scoring scale (weak 1+, mild 2+, moderate 3+, strong 4+) and images were taken using a Zeiss Axiovert 200M microscope (Carl Zeiss Microimaging, Thornwood, NY). For mouse xenograft tumors, biotinylated –

LIV-1 antibody and the Bond Intense R Detection kit (Leica Microsystems, Germany) were used.

**Quantitative Flow Cytometry**. Cell surface LIV-1 expression levels were measured using QIFIKIT flow cytometric indirect immunofluorescence assay (Dako A/S) using mLIV-14 as the primary antibody. 5 x $10^5$ cells/sample were incubated with a saturating concentration (10 µg/ml) of primary antibody for 60 minutes at 4°C. After washes, FITC-conjugated secondary antibody (1:50 dilution) was added for 45 minutes at 4°C. Fluorescence was analyzed by flow cytometry and specific antigen density was calculated based on a standard curve of log geometric mean fluorescence intensity versus log antigen binding capacity.

**Competition binding**. 1 x $10^5$ LIV-1 expressing 293F cells in PBS were aliquotted in each well of 96-well v-bottom plates on ice. The cells were incubated for 1 hour with 5nM AlexaFluor-647 labeled hLIV22 and increasing concentrations (from 0.03 nM to 500 nM) of unlabeled mLIV22, hLIV22 or SGN-LIV1A. Cells were pelleted and washed 2 times with PBS. The cells were then pelleted and resuspended in 125 µL of PBS/FBS . Fluorescence was analyzed by flow cytometry, using percent of saturated fluorescent signal to determine percent labeled mLIV22 bound and to subsequently extrapolate the $IC_{50}$ by fitting the data to a sigmoidal dose-response curve with variable slope.

**Conjugation of antibodies.** The hLIV22-vcMMAE ADC was prepared by partial reduction of antibody interchain disulfide bonds with Tris(2-carboxyethyl)-phosphine (TCEP) followed by conjugation to maleimidocaproylvaline-citrulline-p-aminobenzyloxycarbonyl-MMAE (vcMMAE) as described(16) with the following modifications. Partial reduction of the interchain disulfide bonds, to an average of 2

reduced disulfide bonds or 4 reactive thiols per antibody, was achieved by incubating antibody solutions with 2.5 molar equivalents of TCEP at 37°C in the presence of 1 mmol/L diethylenetriaminepentaacetic acid for 1.5 hours. Final drug loading was determined by reverse phase high-performance liquid chromatography under reducing conditions and by hydrophobic interaction chromatography(16).

**Fluroescence Microscopy.** ADC Internalization Images: MCF7 cells were plated on Fibronectin coated 8 well chamber slides (BD Biosciences) and allowed to grow for 2 days at 37°C in appropriate media. Cells were then incubated with 1ug/ml SGN-LIV1A with or without 10uM chloroquine for 0, 4, or 24 hrs at 37°C. Cells were fixed and permeabilized using Cytofix/Cytoperm solution (BD Biosciences). ADC was detected with goat anti-human IgG Alexafluor 488 (Invitrogen). LAMP1 a lysosomal marker, was detected with biotinylated mouse anti-human CD107a (BD Biosciences), followed by Alexafluor 594 conjugated streptavidin (Invitrogen). Cells were mounted in Prolong Gold Antifade with DAPI (Invitrogen). Images were acquired with a 63x oil objective on an Axiovert 200M inverted fluorescence microscope.Microtubule Network Images. MCF7 cells were plated on D-lys coated 8 well chamber slides (BD Biosciences) and allowed to grow for 2 days at 37°C in appropriate media. Cells were then incubated with 1ug/ml or 10ng/ml SGN-LIV1a for 0 or 24 hrs at 37°C. Cells were fixed as described above. Tubulin was deteted with mouse anti-αtubulin Alexafluor 488 (Invitrogen). Cells were mounted in Slowfade with DAPI (Invitrogen). Images were acquired with a 63x oil objective on an Axiovert 200M inverted fluorescence microscope.

**Cytotoxicity assay.** Tumor cells were incubated with SGN-LIV1A or hLIV22 for 96 hours at 37$^{o}$C. Cell viability was measured by CelltiterGlo (Promega Corporation,

Madison, WI, USA) according to the manufacturer's instructions. Cells were incubated for 25 minutes at room temperature with the CellTiterGlo reagents and luminescence was measured on a Fusion HT fluorescent plate reader (Perkin Elmer, Waltham, MA, USA). Results are reported as $EC_{50}$, the concentration of compound needed to yield a 50% reduction in viability compared with vehicle-treated cells (control=100%).

**PK methods.** Six BALB/c mice were dosed IV with 3 mg/kg of SGN-LIV1A. Blood samples were drawn from the saphenous vein from alternating sub-groups of three mice at 5 minutes, 6 and 24 hours, 2, 4, 7, 10 and 14 days post dose and processed to plasma. Samples were analyzed in a plate based assay as follows: wells were coated overnight with a solution (0.5µg/mL in 0.05M carb/bicarb buffer, pH 9.6) of anti-human IgG kappa antibody (Antibody solutions #AS75-P). After washing with PBS-T, wells were blocked with 1% BSA for 1 hour at room temperature. After washing blocked plates with PBS-T, wells were incubated with samples at room temperature. After 1 hour, plates were washed with PBS-T and incubated for an additional hour with HRP-F(ab')2 goat anti-human IgG Fc-gamma specific (Jackson # 109-036-098). Following a final wash step, TMB substrate was added and incubated for 10 minutes before quenching with 1N HCL, A450 was read and used to calculate serum antibody concentration

***In vivo* activity studies.** Tumor volume was calculated using the formula, $(A \times B^2)/2$, where A and B are the largest and second largest perpendicular tumor dimensions, respectively. Mean tumor volume and weight of mice were monitored and mice terminated when the tumor volume reached 1,000 $mm^3$.

For MCF7-NCI and BR0555 studies, NOD.Cg-Prkdc$^{scid}$ Il2rg$^{tm1Wjl}$/SzJ mice (NSG) (Jackson Labs, Bar Harbor, ME) were implanted subcutaneously with 17β Estradiol 90

day time release tablets (Innovative Research of America, Sarasota FL). Animals were allowed 2 to 6 days recovery time from tablet implant before receiving cell or tissue implant. 17β Estradiol tablets were implanted every 90 days thereafter.

MCF7-NCI cells were implanted at $5x10^6$ / 200µl Matrigel HC25% (BD Biosciences, San Jose, CA). Once tumors reached a mean tumor volume of $100mm^3$, mice were treated by intraperitoneal injection every four days for a total of four doses with either SGN-LIV1A (1 or 3 mg/kg) or human IgGvcMMAE (hIg-vcMMAE) as a non-binding control. An additional group of tumor-bearing mice ($n$ = 5) was left untreated as a control.

BR0555 is a sub-cutaneous model derived from a patient with primary breast cancer (Jackson Labs, Sacramento, CA). NSG mice bearing tumors between 500 and 750 $mm^3$ were sacrificed and the tumors were removed using aseptic technique. Tumors were sectioned into small fragments approximately 3-5$mm^3$ and loaded into 14 gauge trocars. Mice were implanted subcutaneously in the right lateral flank and returned to a clean home box. Implanted mice were monitored once a week and started on study when their tumor reached approximately $250mm^3$. In this model, mice enrolled to the study in a patient accrual fashion; days 58 through 78, and dosing started. At each evaluation, the available cohort of mice was distributed to study groups in an equal fashion with an n=10 per group. Mice were treated by intraperitoneal injection every four days for a total of four doses with either SGN-LIV1A (1 or 3 mg/kg) or human IgGvcMMAE (hIg-vcMMAE) as non-binding control. An additional group of tumor-bearing mice was left untreated as a control.

In the HeLa (ATCC®CLL-2™) *in vivo* study, female Athymic Nude-*Foxn1*$^{nu}$ (Harlan, Livermore CA) were implanted with tissue fragments of tumors maintained in serial passage. Tumors were sectioned into small fragments approximately 3–5mm$^3$ and loaded into 14 gauge trocars. Mice were implanted subcutaneously in the right lateral flank and returned to a clean home box. On day ten post implant, the mice were evaluated and randomly placed into study groups ($n$=8) with a mean tumor size of approximately 100mm$^3$ and dosing was started. Mice were treated by intraperitoneal injection every four days for a total of four doses with either SGN-LIV1A (1 or 3 mg/kg) or human IgGvcMMAE (hIg-vcMMAE) as non-binding control. An additional group of tumor-bearing mice was left untreated as a control.

## Results

**LIV-1 is highly expressed in solid tumors of different origins.** LIV-1 expression was evaluated in human normal tissue and tumor microarrays and in sets of larger tissue sections. LIV-1 is frequently expressed in breast, prostate and melanoma, even in patients previously treated with hormonal therapies (Table 1, Figure 1). By contrast, ovarian, uterine, and lung cancers have measurable, but less frequent, LIV-1 expression. An extensive panel of normal human tissues were also examined and showed limited LIV-1 expression (Table 2, Figure 1). The normal tissues that stain positive for LIV-1 expression in IHC have variable expression. In breast tissue, 0-50% of the cells stain with an intensity of 1-2 on the same scale used for the neoplastic tissue. In prostate tissue, 50-100% of the cells stain with an intensity of 2-4. In testicular tissue, about 50% of the cells stain with an intensity up to 1. The broad expression of LIV-1 in breast, prostate and melanoma tumors, coupled with the restricted normal tissue expression (breast, prostate, and testis) demonstrate that LIV-1 is a target well-suited for an antibody-drug conjugate therapeutic. The expression is most prominent in breast cancer, the focus of this study.

**LIV-1 is highly expressed in post-hormone treated primary and metastatic breast tumors.** To determine the expression of LIV-1 in breast carcinomas, a murine anti-LIV-1 mAb was used for the detection in formalin-fixed paraffin-embedded (FFPE) samples by immunohistochemistry. We found that large sections of tumor samples provided better measure of LIV-1 expression in the tumor samples analyzed compared to commercially available tumor microarrays.

Since there is known positive correlation between LIV-1 expression and estrogen receptor, we also evaluated breast tumor samples where the patients had previously

received hormone therapy for their ER+ cancers. We analyzed expression in breast cancer biopsies in patients having received hormonal therapy (tamoxifen or aromatase inhibitors). A total of 82 post-hormone therapy biopsies were studied and 88% of these expressed LIV-1 (at any level of intensity or % positive). As illustrated in Figure 1A, 92% of primary site post-hormone treated tumor biopsies expressed LIV-1 with intensity of the staining ranging from weak (1-2+) to strong (3-4+). About 50% of the cases had ≥50-100% of tumor cells expressing LIV-1. Good concordance was observed with the reactivity of another anti-LIV-1 mAb in formalin-fixed tissues (data not shown). The immunostaining pattern was characterized as both membranous and cytoplasmic. The staining was LIV-1 specific, based on concordant reactivity between the two anti-LIV-1 mAbs used and the absence of staining with an isotype-matched negative control antibody. We also studied post-hormonal therapy metastatic breast tumor biopsies. 18 out of 23 cases (78%) expressed LIV-1, with ~75% of cases staining ≥50-100% of the tumor cells (Figure 1B).

Expression of LIV-1 in triple negative (ER-, PgR-, Her-2 unamplified) primary breast tumors was also evaluated. We observed 65% LIV-1+ in a set of 20 cases, with 40% (8/20) showing ≥50-100% of tumor cells positive, albeit with lower intensity of LIV-1 expression (Figure 1C) compared to ER+ cases. Representative images of staining intensity are shown in Figure 1D.

**Quantitative flow cytometric analysis of LIV-1 expression on human cancer cell lines.** Cell surface expression of LIV-1 in human tumor cell lines was evaluated using quantitative flow cytometry. The panel of cell lines included breast, cervical, head and

neck, hepatocellular, kidney, ovarian, pancreatic, prostate, and melanomas. The highest level of LIV-1 expression was observed in the MCF-7 breast cancer cell line from ATCC (175,000 sites/cell) while ZR-75-1(ATCC® CRL-1500™) had about 80,000 sites/cell (Table 3). Other cell lines (ovarian, pancreatic, head and neck, melanomas) showed moderate to low level expression of LIV-1 by qFACS.

**Humanized LIV-22 affinity.** Parental murine LIV22 (mLIV22) was humanized to hLIV22 using the complementary determining region (CDR) grafting method. To ensure that neither humanization nor conjugation minimal effects on binding to LIV-1, the binding affinity of mLIV22 was compared with hLIV22 and SGN-LIV1A in a competition binding assay. The half-maximal inhibitory concentrations ($IC_{50}$) determined for mLIV22, hLIV22 and SGN-LIV1A were 3.5, 4.6 and 5.6nM, respectively. These data suggest that humanization did not significantly impact the binding affinity of hLIV22 to LIV-1.

**Anti-LIV-1 ADCs are potent inhibitors of cell proliferation of MCF-7 breast carcinoma cells.** The humanized LIV-1 antibody (hLIV-22) was conjugated to the anti-tubulin drug, vcMMAE, on reduced cysteines usually involved in interchain disulfide bonds with a mean stoichiometry of 4 drugs/antibody(16). The resulting ADC, SGN-LIV1A, has a potent cytotoxic activity against MCF-7 cell line (ATCC) with an $EC_{50}$ value of 6.3 ng/ml in a CellTiter Glo (Promega) cytotoxicity assay (Figure 2B). In contrast, neither unconjugated parental antibody (Figure 2) nor an ADC control hIgG-vcMMAE showed substantial cytotoxic activity ($EC_{50}$ > 10,000 ng/ml) (data not shown). In this assay, maximum cytotoxicity was 70%. When comparing a MCF-7 cell lines from different sources we found they had varying concentrations of antigen on the surface of

their plasma membrane. We have shown decreasing amounts of antigen displayed on the surface of the cell has an adverse effect on *in vitro* cytotoxicity (supl. Table 1) of SGN-LIV1A. Incomplete cell killing with SGN-LIV1A could be due to a heterogeneous low antigen expressing or quiescent, slowly dividing cell subpopulation.

**SGN-LIVA engages the target, internalizes and traffics to the lysosome.** Subcellular localization of SGN-LIV1A in MCF-7 cells (a LIV-1 positive cell line) was examined by fluorescence microscopy at 0, 4, and 24 hours. SGN-LIV1A internalizes slowly over a 24 hour period (Figure 3A, top panels). To better visualize SGN-LIV1A accumulation within lysosomes, cells were treated with 10 μM chloroquine to block ADC degradation (Figure 3A, bottom panels). Non-binding control ADC showed minimal binding and internalization into MCF-7 cells, with or without chloroquine (data not shown). A control non-lysosomal ADC internalized, but did not converge on the lysosome with 10uM chloroquine treatment, suggesting the SGN-LIV1A lysosomal localization is not simply a collapse of intracellular vesicles (data not shown). In summary, SGN-LIV1A internalizes throughout a 24 hour treatment period and traffics to the lysosome where proteolytic release of the cytotoxic payload occurs.

**Disruption of Microtubules.** Treatment of LIV-1 expressing MCF-7 cells with SGN-LIV1A at doses as low as 10 ng/mL for 24 hours induced disruption of the microtubule network (Figure 3B). At 24hours 49% (N=150) (Figure 2) of cells treated with 1μg/ml SGN-LIV1a or 16% (N=100) of cells treated with 10ng/ml SGN-LIV1a displayed condensed chromosomes and abnormal spindles. At 24hrs 0% (N=300) of cells treated with non-binding control displayed this phenotype. These data are consistent with the proposed mechanism of action leading to mitotic arrest.

**PK and *in vivo* ADC activity study using MCF-7, BR0555 and HeLa tumors.** To measure the pharmacokinetic properties of SGN-LIV1A, a single 3 mg/kg dose was administered IV to BALB/C mice; blood samples were taken out to 14 days. The pharmacokinetic properties of the total antibody appear consistent with a two compartment model (Figure 4A). The terminal half-life, calculated using non-linear regression, is 6.8 days.

The antitumor activity of SGN-LIV1A was evaluated in xenograft models of breast, and cervical lineage. Two different breast cancer models were explored, one using MCF-7 cells and the other using a patient-derived tissue model. In the MCF-7 breast cancer cell xenograft model, tumor regressions were achieved with four 3mg/kg doses of SGN-LIV1A given every four days (q4dx4; Figure 4B), well below the mean tolerated dose of 10mg/kg in rodents. While tumor growth delay was seen when dosing with the non-targeted ADC, when comparing it to the 3 mg/kg SGN-LIV1A dose group , P-values compute to $<0.05$, meeting the threshold of statistical significance difference and indicating both a dose response and immunologic specificity of the targeted therapeutic. ADC activity in the absence of target has been documented previously on a number of antibody backbones and chemotype combinations(17-19). Non-cancer antigen dependent activity is a continuing topic of study and has been attributed to a combination of factors including the enhanced permeability and retention effect of a tumor, ADC and drug linker stability, cellular susceptibility to the delivered cytotoxin, and relative cell permeability of the released drug.

The second breast cancer model (BR0555) was derived from the ER+, PR+ and HER2- infiltrating breast ductal carcinoma tumor from an 86-year-old Caucasian patient

prior to any therapeutic intervention. Treatment of BR0555 tumor bearing mice with SGN-LIV1A on a q4dx4 schedule showed antitumor activity, resulting in pronounced tumor regressions (Figure 4C).

SGN-LIV1A activity was also examined in the HeLa (cervical cancer-derived) xenograft model. Treatment with four 3 mg/kg doses of SGN-LIV1A given every 4 days resulted in significant tumor shrinkage compared to a non-binding control ADC (Figure 4D).

**Discussion:**

Antibody-drug conjugates directed towards tumor specific antigens are clinically proven as effective treatments of both solid and liquid tumors. We have shown in this study that LIV-1, an integral cell surface membrane protein, is a promising candidate for ADC therapy due to its broad expression in a number of cancer indications and limited normal tissue expression. LIV-1 is expressed across an array of cell lines from various lineages with surface copy numbers ranging from >170,000 to >5,000. Further, inspection of archived biopsies showed a high percentage of primary, metastatic, and triple-negative breast cancer tissues that expressed the antigen. Based on these encouraging findings we engineered a humanized anti-LIV-1 antibody that binds specifically to the extracellular domain of LIV-1, internalizes after antigen binding and traffics to the lysosome. Using this antibody, we designed and generated SGN-LIV1A which leverages the specificity of the antibody and the activity of a potent microtubule-disrupting agent (MMAE) to produce a LIV-1 directed cytotoxic agent. SGN-LIV1A shows *in vitro* and *in vivo* potency and specificity when treating LIV-1 expressing cell lines and tumors.

*In vitro* assays showed that high LIV-1 expressing cell line was insensitive to treatment with the naked antibody alone. Cell lines that have low LIV-1 cell surface copy number are resistant to SGN-LIV1A and only show growth inhibition at concentrations >1,000 ng/mL.

We have shown that SGN-LIV1A is effective in *in vivo* xenograft models of different origin including models of breast, prostate, and cervical lineage, delaying tumor growth at a relatively low dose (1 mg/kg/dose). Consistent with the proposed mechanism of ADC

action, SGN-LIV1A was most effective *in vivo* on xenograft models with the highest expression of LIV-1, showing pronounced tumor regressions at doses of 3 mg/kg, while the antibody alone did not inhibit tumor growth at doses as high as 30 mg/kg. Cell surface LIV-1 copy number is difficult to accurately ascertain for tissues. However, IHC staining of xenograft sections indicates homogenous LIV-1 levels (100% of the cells) at an intensity of 2-3, which is equivalent or less than the staining seen in over 50% of the metastatic breast biopsy sections.

Dependent upon the tumor receptor expression profile, there are now several targeted therapeutic approaches that can be used, including HER2 and hormone-directed regimens. However, regardless of their classification, patients who have relapsed with distant stage metastatic breast cancer have no curative therapeutic options open and face a 5-year survival rate of 24% (20). Current systemic treatments of these patients aim to prolong survival, control disease progression, alleviate symptoms and enhance patient quality of life. In this study we have shown that LIV-1 is expressed in all subtypes of breast cancer (including triple-negative) and that SGN-LIV1A is active as a single agent in preclinical models. These data in combination with the recent successes of ADCs supports pursuing SGN-LIV1A as a new therapeutic modality for refractory metastatic breast cancer and other LIV-1 positive indications.

**Acknowledgments:** the authors would like to thank Jonathan Drachman for his careful review and assistance in completing this manuscript.

## References

1. Sievers EL, Senter PD. Antibody-drug conjugates in cancer therapy. Annual review of medicine. 2013;64:15-29.
2. Taylor KM, Morgan HE, Johnson A, Hadley LJ, Nicholson RI. Structure-function analysis of LIV-1, the breast cancer-associated protein that belongs to a new subfamily of zinc transporters. Biochem J. 2003;375:51-9.
3. Lopez V, Kelleher SL. Zip6-attenuation promotes epithelial-to-mesenchymal transition in ductal breast tumor (T47D) cells. Experimental cell research. 2010;316:366-75.
4. Manning DL, Daly RJ, Lord PG, Kelly KF, Green CD. Effects of oestrogen on the expression of a 4.4 kb mRNA in the ZR-75-1 human breast cancer cell line. Mol Cell Endocrinol. 1988;59:205-12.
5. Yamashita S, Miyagi C, Fukada T, Kagara N, Che YS, Hirano T. Zinc transporter LIVI controls epithelial-mesenchymal transition in zebrafish gastrula organizer. Nature. 2004;429:298-302.
6. Lue HW, Yang X, Wang R, Qian W, Xu RZ, Lyles R, et al. LIV-1 promotes prostate cancer epithelial-to-mesenchymal transition and metastasis through HB-EGF shedding and EGFR-mediated ERK signaling. PloS one. 2011;6:e27720.
7. Zhao L, Chen W, Taylor KM, Cai B, Li X. LIV-1 suppression inhibits HeLa cell invasion by targeting ERK1/2-Snail/Slug pathway. Biochemical and biophysical research communications. 2007;363:82-8.
8. Unno J, Satoh K, Hirota M, Kanno A, Hamada S, Ito H, et al. LIV-1 enhances the aggressive phenotype through the induction of epithelial to mesenchymal transition in human pancreatic carcinoma cells. International journal of oncology. 2009;35:813-21.
9. Taylor KM, Hiscox S, Nicholson RI. Zinc transporter LIV-1: a link between cellular development and cancer progression. Trends in endocrinology and metabolism: TEM. 2004;15:461-3.
10. Huber MA, Kraut N, Beug H. Molecular requirements for epithelial-mesenchymal transition during tumor progression. Current opinion in cell biology. 2005;17:548-58.
11. Manning DL, Robertson JF, Ellis IO, Elston CW, McClelland RA, Gee JM, et al. Oestrogen-regulated genes in breast cancer: association of pLIV1 with lymph node involvement. Eur J Cancer. 1994;30A:675-8.
12. Dressman MA, Walz TM, Lavedan C, Barnes L, Buchholtz S, Kwon I, et al. Genes that co-cluster with estrogen receptor alpha in microarray analysis of breast biopsies. Pharmacogenomics J. 2001;1:135-41.
13. Tozlu S, Girault I, Vacher S, Vendrell J, Andrieu C, Spyratos F, et al. Identification of novel genes that co-cluster with estrogen receptor alpha in breast tumor biopsy specimens, using a large-scale real-time reverse transcription-PCR approach. Endocr Relat Cancer. 2006;13:1109-20.
14. Doronina SO, Toki BE, Torgov MY, Mendelsohn BA, Cerveny CG, Chace DF, et al. Development of potent monoclonal antibody auristatin conjugates for cancer therapy. Nature biotechnology. 2003;21:778-84.
15. Kabat EA, National Institutes of Health (U.S.). Sequences of proteins of immunological interest. 5th ed. Bethesda, Md.
Washington, D.C.: U.S. Dept. of Health and Human Services, Public Health Service

For sale by U.S. G.P.O.; 1991.
16. Lyon RP, Meyer DL, Setter JR, Senter PD. Conjugation of anticancer drugs through endogenous monoclonal antibody cysteine residues. Methods in enzymology. 2012;502:123-38.
17. Sharman JP, Oki Y, Advani RH, Bello CM, Winter JN, Yang Y, et al. A Phase 2 Study Of Brentuximab Vedotin In Patients With Relapsed Or Refractory CD30-Positive Non-Hodgkin Lymphomas: Interim Results In Patients With DLBCL and Other B-Cell Lymphomas2013.
18. Boghaert ER, Khandke K, Sridharan L, Armellino D, Dougher M, Dijoseph JF, et al. Tumoricidal effect of calicheamicin immuno-conjugates using a passive targeting strategy. International journal of oncology. 2006;28:675-84.
19. Kovtun YV, Audette CA, Ye Y, Xie H, Ruberti MF, Phinney SJ, et al. Antibody-drug conjugates designed to eradicate tumors with homogeneous and heterogeneous expression of the target antigen. Cancer research. 2006;66:3214-21.
20. Howlader N, Noone A, Krapcho M, Garshell J, Neyman N, Altekruse S, et al. SEER Cancer Statistics Review, 1975-2010. In: Institute NC, editor. Bethesda, MD2013.

List of Tables:

Author Manuscript Published OnlineFirst on September 24, 2014; DOI: 10.1158/1535-7163.MCT-13-0896
Author manuscripts have been peer reviewed and accepted for publication but have not yet been edited.

Table 1: LIV-1 expression in multiple cancer types

| Neoplastic Tissue | Number of Positive Samples | Number of Samples Examined | % Positive |
|---|---|---|---|
| Breast | 88 | 95 | 93 |
| Melanoma | 42 | 51 | 82 |
| Prostate | 36 | 50 | 72 |
| Ovary | 10 | 21 | 48 |
| Uterus | 6 | 20 | 30* |
| Lung | 3 | 30 | 10* |

Table 2: LIV-1 expression in normal tissue

| **Normal Tissues Negative for Anti-LIV-1 Staining** | | |
|---|---|---|
| Adrenal gland | Kidney | Skin |
| Bone | Larynx | Spleen |
| Cerebellum and Cerebrum | Liver | Stomach |
| Colon | Lung | Striated muscle |
| Esophagus | Mesothelium | Thymus gland |
| Eye | Ovary | Thyroid |
| Heart | Parathyroid gland | Tonsil |
| Hypophysis | Salivary gland | Uterine Cervix |
| Intestine | | |
| Normal Tissues Positive for Anti-LIV-1 Staining | | |
| Breast | Testis | |
| Prostate | | |

Table 3: quantitative flow data showing LIV-1 expression on cell lines of various origins

| Cell Line Name | Source | LIV-1 Copy # |
|---|---|---|
| MCF-7 (ATCC) | Breast | 175000 |
| ZR-75-1 | Breast | 91000 |
| DU-4475 | Breast | 50000 |
| BT-20 | Breast | 46000 |
| MDA-MB-157 | Breast | 45000 |
| MDA-MB-175-VII | Breast | 39000 |
| BT483 | Breast | 36000 |
| MDA-MB-231 | Breast | 32000 |
| T47D | Breast | 25000 |
| MCF-7 (nci) | Breast | 22000 |
| HeLa | Cervical | 78000 |
| Detroit 562 | Head and Neck | 22000 |
| Hep3B | hepatocellular | 32000 |
| HEK293F | Kidney | 59000 |
| SKOV3 | ovarian | 71000 |
| ES-2 | ovarian | 38000 |
| OVCAR-3 | ovarian | 34000 |
| HupT3 | Pancreatic | 27000 |
| PC-3 | Prostate | 35000 |
| LNCAP | Prostate | 32000 |
| 22RV-1 | Prostate | 23000 |
| SKMEL-5 | Melanoma | 29000 |
| G361 | Melanoma | 25000 |
| A2058 | Melanoma | 16000 |
| WM115 | Melanoma | 12000 |
| Hs695T | Melanoma | 22000 |
| Sk-Mel-2 | Melanoma | 19000 |
| MALME-3M | Melanoma | 15000 |
| Skmel3 | Melanoma | 24000 |
| CHL1 | Melanoma | 16000 |
| HNCB | Melanoma | 6000 |

**Figure legends:**

**Fig. 1 A-D** LIV-1 is expressed in primary and metastatic post-hormone treated breast cancer cases. Tissue sections were preserved in formalin, expression was detected using Fast Red as a substrate for alkaline phosphatase. A) 54 of 59 (92%) of post-treatment, primary site breast cancer biopsies express LIV-1. B) 18 of 23 (78%) of post-treatment, metastatic breast cancer biopsies express LIV-1. C) 13 of 20 (65%) of primary site triple negative breast cancer biopsies express LIV-1. D) Examples of tissues with LIV-1 specific staining intensity of 1-4.E) Examples of normal tissue staining, clockwise from top left: lung, colon, prostate, breast

**Fig. 2 A-B** hLIV-22 retains binding affinity and has potent *in vitro* cytotoxicity activity as a conjugate. A) FACS based competition binding experiments, performed by titrating unlabeled test article into cells with a constant concentration of labeled mLIV22 present, showed no post-humanization loss of affinity. B) MCF-7 ATCC cells were grown in 96 well plates, SGN-LIV1A or naked hLIV-22 were added for 96 hours prior to monitoring viability using CellTiter Glo

**Fig. 3 A-B** SGN-LIV1A internalizes, traffics to the lysosome and disrupts the microtubule network in LIV-1 expressing cells. A) Top panels: SGN-LIV1A treated cells, arrows point to internalized ADC. Bottom panels: SGN-LIV1A + Chloroquine treated cells. ADC is stained green, LAMP 1 a lysosome associated proteins is stained red, areas of co-localization show as orange. B) Top panels: Cells are incubated with non-binding control ADC for 0 and 24 hours. Bottom panels: Cells are incubated with SGN-LIV1A for 0 and 24 hours. Microtubules are stained green and DNA is stained blue.

**Fig. 4 A-D** PK and *In vivo* model activity of SGN-LIV1A. A) The pharmacokinetic properties of the total antibody appear to follow a two compartment model, top panel. The terminal half-life, calculated using non-linear regression, is 6.8 days, bottom panel. B) NSG mice were implanted s.c. with MCF-7 NCI cells. Once tumors reached 100 $mm^3$, animals were treated with indicated doses of SGN-LIV1A or a non-binding control every four days, a total of four times. C) NSG mice were implanted with fragments of BR0555 tumors, once tumors reached 250 $mm^3$ they were treated as in (B). D) Nude mice were implanted with HeLa cells and treated as in (B)

Author Manuscript Published OnlineFirst on September 24, 2014; DOI: 10.1158/1535-7163.MCT-13-0896
Author manuscripts have been peer reviewed and accepted for publication but have not yet been edited.

# Figure 1 LIV-1 expression in breast cancer and normal tissue

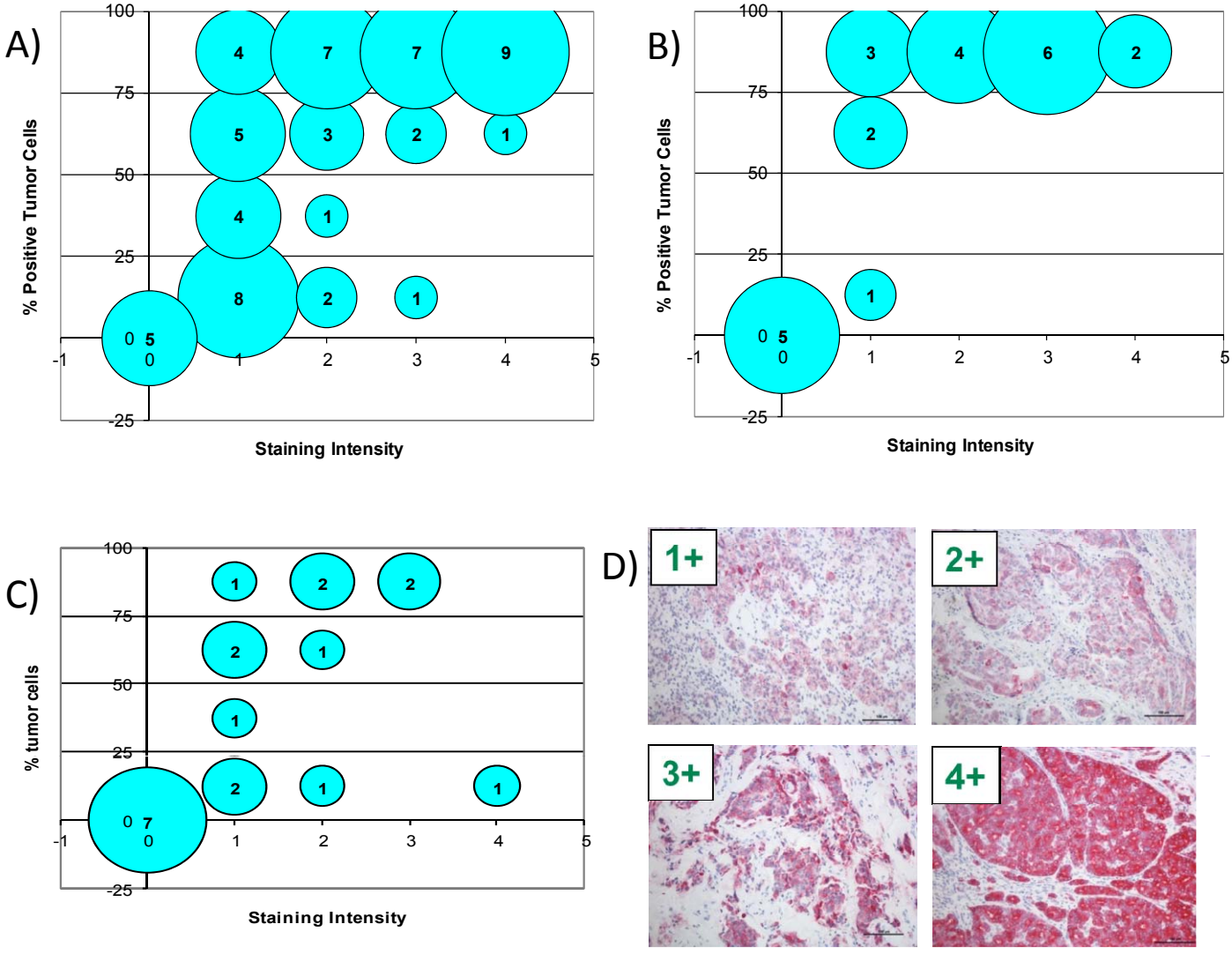

Figure 2. Binding affinity and *in vitro* cytotoxicity measurements

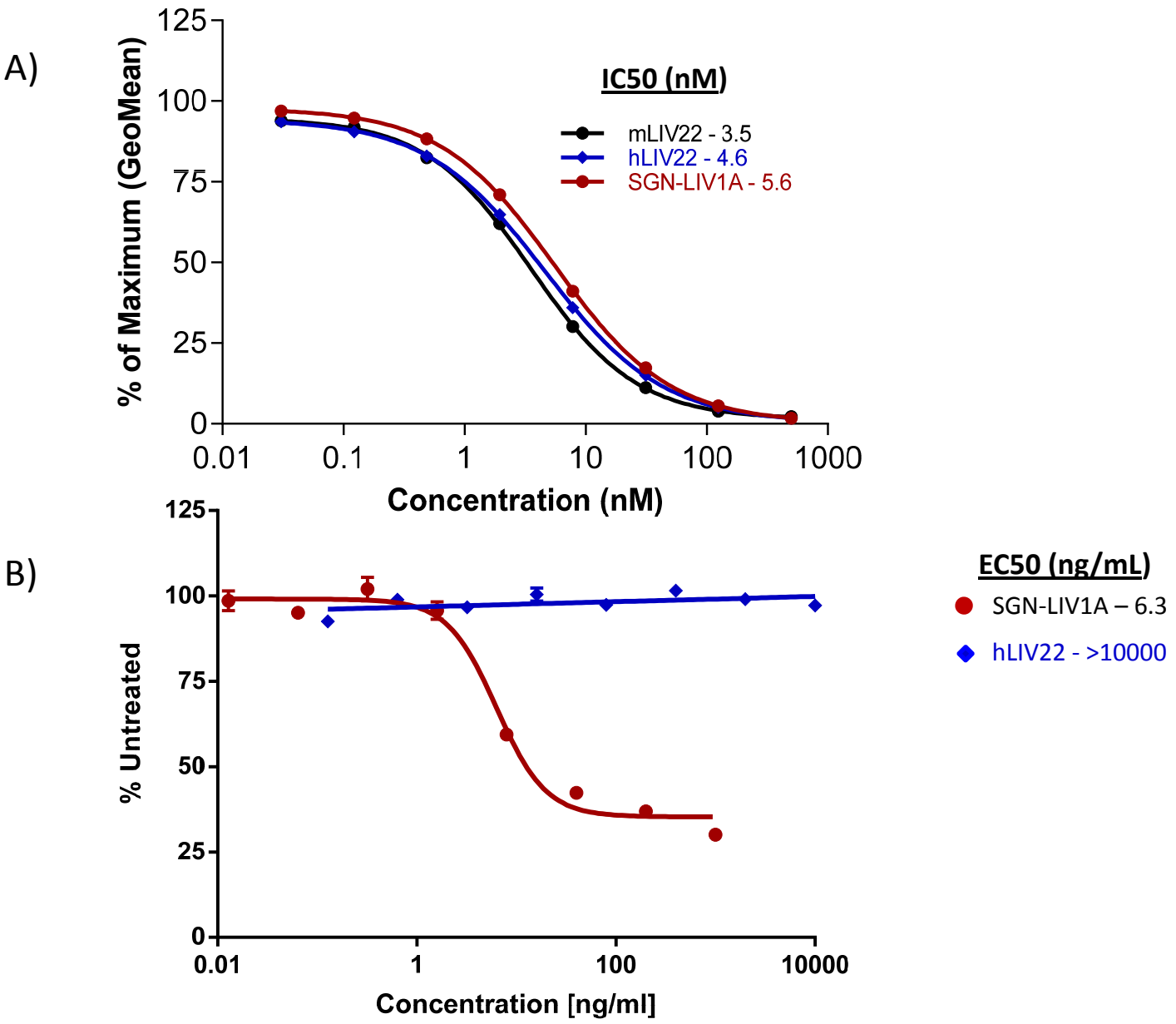

Figure 3: Fluorescence imaging of ADC internalization and disruption of microtubule network

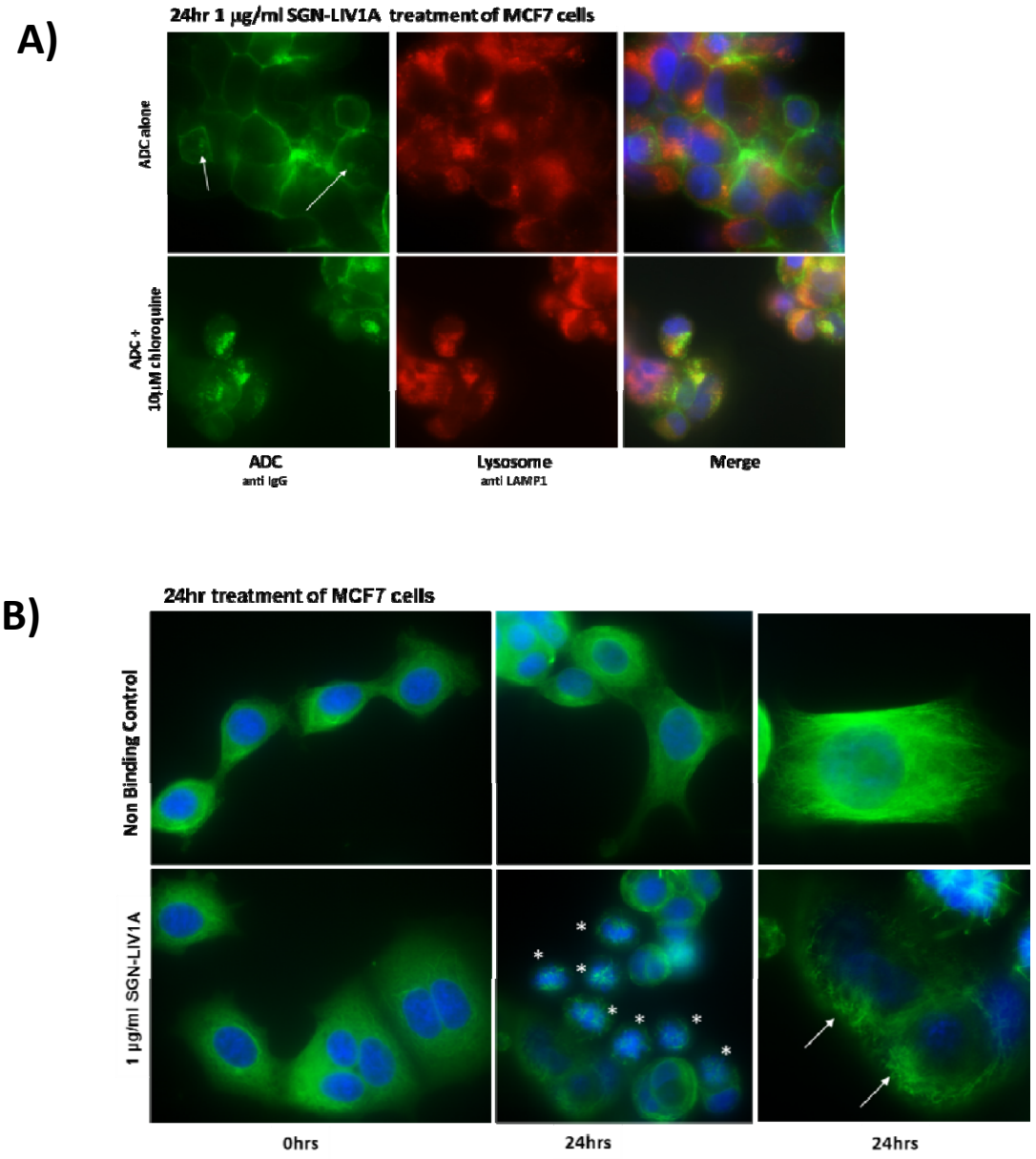

Figure 4: PK and In vivo models

A)

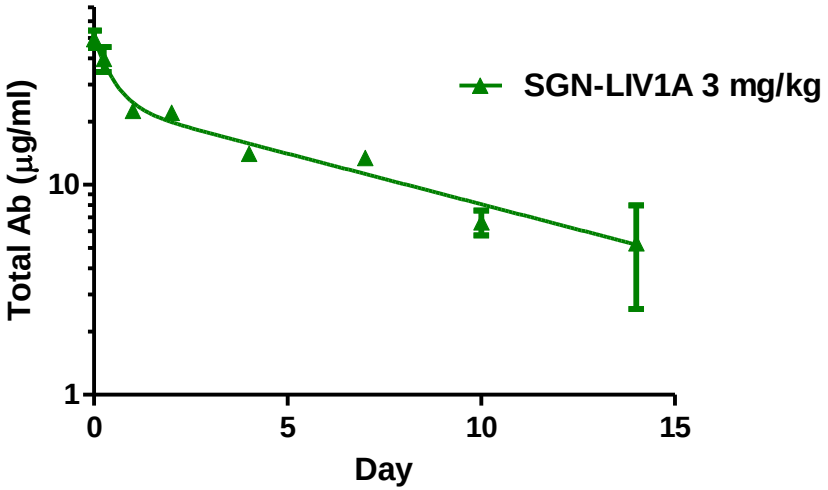


C) BR0555

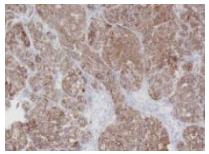

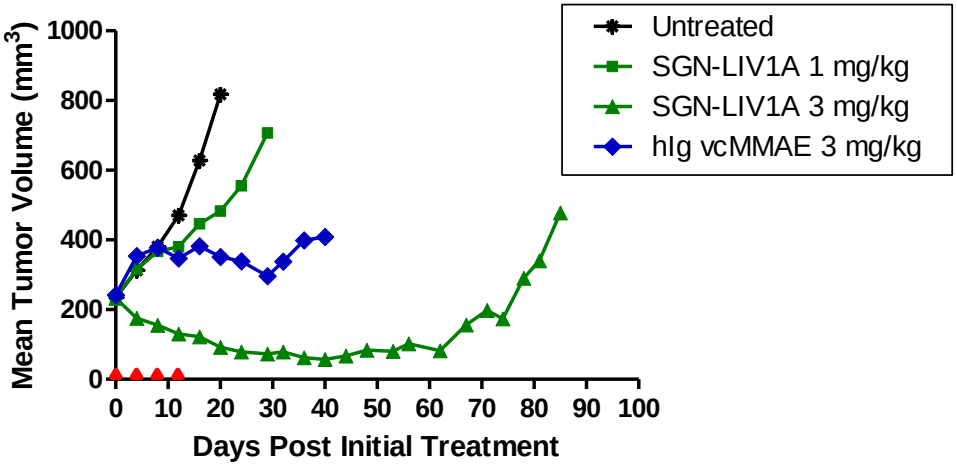


B) MCF-7 (NCI)

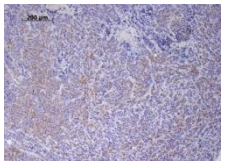

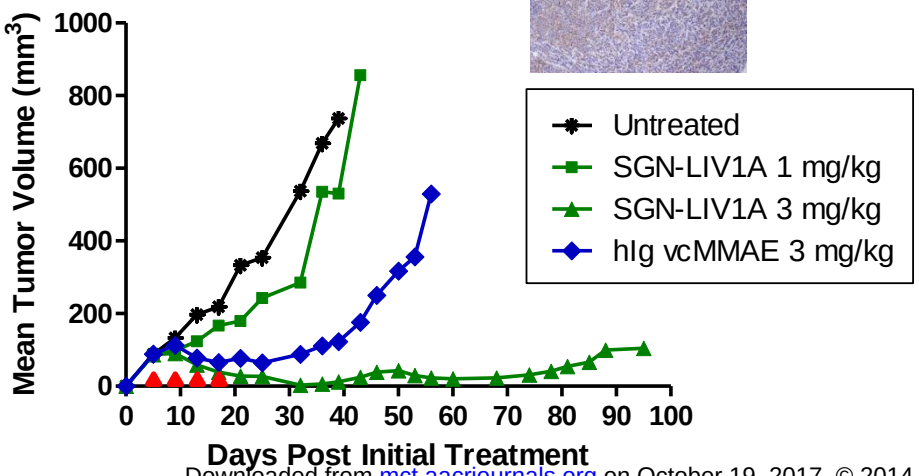


D) HeLa

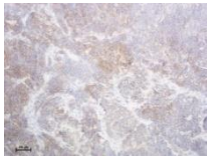

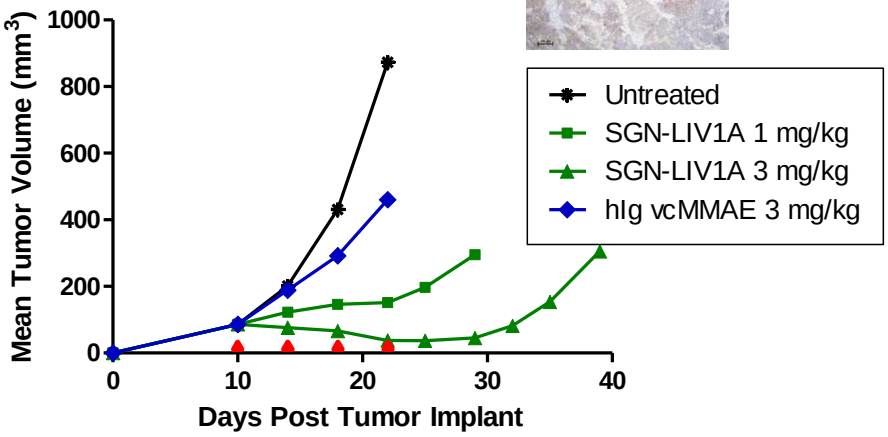

AACR American Association for Cancer Research

Molecular Cancer Therapeutics

# SGN-LIV1A: A Novel Antibody-Drug Conjugate Targeting LIV-1 for the Treatment of Metastatic Breast Cancer

Django Sussman, Leia M Smith, Martha E. Anderson, et al.

*Mol Cancer Ther* Published OnlineFirst September 24, 2014.